

# A DUAL ALGORITHM FOR NON-ABELIAN YANG-MILLS COUPLED TO DYNAMICAL FERMIONS

J. WADE CHERRINGTON<sup>1</sup>

<sup>1</sup>Department of Applied Mathematics, University of Western Ontario, London, Ontario, Canada  
e-mail: jcherrin@uwo.ca

**ABSTRACT.** We extend the dual algorithm recently described for pure, non-abelian Yang-Mills on the lattice to the case of lattice fermions coupled to Yang-Mills, by constructing an ergodic Metropolis algorithm for dynamic fermions that is local, exact, and built from gauge-invariant boson-fermion coupled configurations. For concreteness, we present in detail the case of three dimensions, for the group  $SU(2)$  and staggered fermions, however the algorithm readily generalizes with regard to group and dimension. The treatment of the fermion determinant makes use of a polymer expansion; as with previous proposals making use of the polymer expansion in higher than two dimensions, the critical question for practical applications is whether the presence of negative amplitudes can be managed in the continuum limit.

## 1. BACKGROUND

Despite continued progress in algorithms and hardware, the inclusion of dynamical fermions in lattice gauge calculations continues to incur significant computational expense. To motivate our proposal for a novel fermion algorithm, we briefly review how dynamical fermions are currently addressed. Recall that dynamic fermions coupled to a gauge field on a  $D$ -dimensional hypercubic lattice for  $D \geq 2$  are governed by an action of the form

$$(1) \quad S[g_e, \psi_v, \overline{\psi}_v] = S_G[g_e] + S_F[g_e, \psi_v, \overline{\psi}_v],$$

where the  $g_e$  are valued in the gauge group  $G$  at the edges of the lattice and  $\psi_v$  are the fermion fields defined at the vertices of the lattice.

Unlike gauge group variables, it is not practical to directly simulate Grassmann variables on the computer. A common approach to dynamical fermion simulation starts by integrating out the fermion variables appearing in  $S_F[g_e, \psi_v, \overline{\psi}_v]$ , to give a function of the gauge variables known as the fermion determinant (its specific form is reviewed in Section 2). The fermion determinant can be combined with the kinetic part of the gauge boson amplitude  $e^{-S_G[g_e]}$  to give an effective action for the gauge variables from which simulations on a computer can in principle proceed. However, the fermion determinant renders this effective action non-local — it couples together gauge variables that are arbitrarily distant in the lattice. This poses a considerable problem for the simulation, since computing the change in the effective action due to a small change in any variable becomes very expensive, growing prohibitively with increasing lattice volume. A variety of algorithms have been devised to work with the fermion determinant; a description of some of the methods commonly employed can be found for example in [6].

After reviewing the description of single component, staggered free fermions in terms of self-avoiding polymers (as was done for example in [9]), we review what happens when a similar procedure is applied to multi-component fermion fields minimally coupled to gauge fields. In this case each polymer configuration corresponds to a Wilson loop functional; i.e. the trace of a product of representation matrices around the polymer. Because there is more than one component of the fermion fields in the non-abelian coupled case, the strict self-avoiding constraint of the single component case is weakened; that is, for an  $n$ -component fermion, up to  $n$  directed polymer lines can enter and leave a given vertex. The picture has long been known — it is essentially that of a hopping parameter expansion of the fermion determinant, described for example in [14]. Unlike many past applications, in the present case no cut-off in the power of the hopping parameter or otherwise is applied. Because we seek an exactly dual model, all polymers are included in the configurations considered.

For each polymer diagram that arises in the free case, upon applying the duality transformation for the group-valued field the result is a sum of configurations consisting of all closed, branched, colored surfaces (spin

foams) with open one-dimensional boundaries defined by the polymer diagram. The totality of spin foams associated with all polymer diagrams (including the trivial empty polymer) defines the joint configuration space. Crucially, local changes to the dual configurations (either polymer or surface structure) lead to local changes in the dual amplitude.

The two theoretical inputs for this construction, a polymer decomposition of the fermion determinant (i.e. hopping parameter expansion as described in [14]) and a dual non-abelian model (e.g. [13] and references therein), have been present in the literature for some time, and as we shall see the construction of the joint dual model at the formal level is a rather straightforward synthesis of these constituent models. However, unlike (the simplest implementations of) conventional lattice gauge simulations, finding *any* practical algorithm for a dual model has proven somewhat non-trivial in the non-abelian case for dimensions greater than two. The algorithm proposed here builds upon the dual non-abelian algorithm of [5] that has recently been tested in the pure Yang-Mills sector. In addition to pure spin foam moves, we construct a set of moves that act on polymer structure and specify the type of vertex amplitudes that arise due to the charges carried by the polymer. Currently, an implementation of this algorithm is being tested and will be reported on in a forthcoming work.

For context, it should be noted that a similar picture was present in the work of Aroca et al. [1] and Fort [7], which dealt with the abelian case of  $U(1)$  and proposed using a Hamiltonian that leads to a different Lagrangian formulation, where the ensemble is built from a restricted subset of the configurations that arise in the Kogut-Susskind case. In future work, we believe the non-abelian generalization of [1] may be a very interesting alternative to the Kogut-Susskind formulation used here, particularly if the imbalance between negative and positive amplitudes and the reduction of species doubling described in [1] can be carried over to the non-abelian case.

The outline of the paper is as follows. In Section 2, we review the origin of the fermion determinant and discuss its expansion in terms of polymers. In Section 3, we briefly review the dual computational framework for non-abelian, pure Yang-Mills theory on the lattice. In Section 4, we show a natural way to combine these frameworks and formulate ergodic moves for the coupled fermion-boson system. In Section 5, we offer some conclusions and describe our program for ongoing numerical work based on this algorithm and its extensions. Appendix A describes the vertex amplitudes that arise in the joint case, while Appendix B expands on Section 2 to describe the trace structure of polymers with multiply occupied vertices.

## 2. POLYMER DESCRIPTION OF FERMIONS ON THE LATTICE

In this section, we start from a conventional lattice discretization of free fermions, following [12] in essentials and notation. In the usual manner, the fermion determinant is arrived at by exact integration of the Grassmann variables. Following [9], the fermion determinant is then expanded into states, each of which is represented by a family of *disjoint, closed oriented loops*, including trivial and degenerate “loops”, the *monomers* and *dimers*, respectively. A typical polymer configuration (in the  $D = 2$  massive case) is illustrated <sup>1</sup> We now review explicitly how the fermion determinant and polymer picture come about. Note this section is purely for pedagogical purposes and to fix notation to be used later; those familiar with the hopping parameter expansion of the fermion determinant can safely skip it.

**2.1. Kogut-Susskind staggered fermions — free case.** To illustrate the concept and introduce terminology, we treat a single species of fermions with no additional indices. We start with the naive lattice field action for free staggered fermions

$$(2) \quad S = \sum_{x \in V} \bar{\Psi}_x (\gamma_\mu \partial_\mu + m) \Psi_x,$$

where  $\gamma_\mu$  are the (Euclidean) Dirac matrices and  $V$  is the set of lattice vertices.

Using the central difference for the partial derivative, this becomes

$$(3) \quad S = \sum_{x \in V} a^D \left\{ m(\bar{\Psi}_x \Psi_x) - \frac{1}{2a} \sum_{\mu=1}^D (\bar{\Psi}_x \gamma_\mu \Psi_{x+\hat{\mu}} - \bar{\Psi}_{x+\hat{\mu}} \gamma_\mu \Psi_x) \right\},$$

---

<sup>1</sup>Figure 1 shows the fermion state on part of a larger lattice to which periodic boundary conditions are applied.

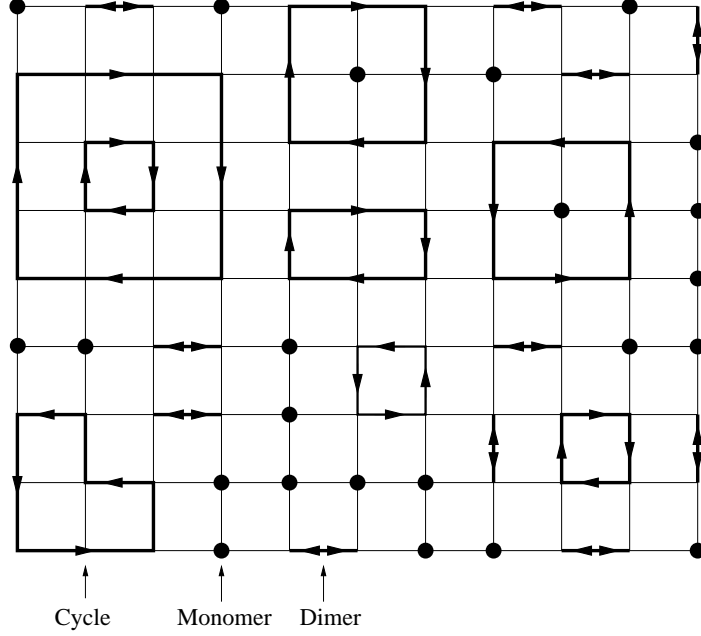


FIGURE 1. Part of a typical configuration in the polymer expansion of the fermion determinant in two dimensions (massive case).

where  $D$  is the dimension<sup>2</sup> of the hyper-cubic lattice,  $m$  is the mass,  $a$  is the lattice spacing, and  $\mu$  labels one of the  $D$  directions of the lattice;  $\hat{\mu}$  is the unit lattice vector associated to the  $\mu$ th direction. Following [12], we change to a basis which diagonalizes the gamma matrices, rewriting the free action as

$$(4) \quad S = \sum_{x \in V} \left\{ M(\bar{\psi}_x \psi_x) - K \sum_{\mu=1}^D \alpha_{x\mu} (\bar{\psi}_x \psi_{x+\hat{\mu}} - \bar{\psi}_{x+\hat{\mu}} \psi_x) \right\},$$

with  $\alpha_{x\mu} \equiv (-1)^{x_1 + \dots + x_{\mu-1}}$  for  $\mu \in \{1, 2, \dots, D\}$  where the  $x_i$  are the components of the lattice site four-vector and  $\frac{M}{2K} = ma$ . The edge dependent sign factor  $\alpha_{x\mu}$  arises from the chosen diagonalization.

To express the result of integration over the Grassmann variables it is convenient to introduce the *quark matrix*  $Q$ , defined in terms of lattice regularized action as

$$(5) \quad S_F[g_e, \psi_v, \bar{\psi}_v] = \sum_{x, y \in V} \bar{\psi}_y Q[g_e]_{yx} \psi_x.$$

For later reference, we include dependence on the gauge degrees of freedom in our definition of  $Q$ . We next apply the well known result [12] that the Grassmann integral over the fermion fields at every vertex evaluates to

$$(6) \quad \int \left( \prod_{v \in V} d\psi_v d\bar{\psi}_v \right) e^{-S_F[g_e, \psi_v, \bar{\psi}_v]} = \int \left( \prod_{v \in V} d\psi_v d\bar{\psi}_v \right) e^{-\sum_{x, y \in V} \bar{\psi}_y Q[g_e]_{yx} \psi_x} = \det Q[g_e],$$

the determinant of the quark matrix.

Next we recall the continuum form of the action for massive fermions coupled to a gauge field. In the massive case, the quark matrix can be written as

$$(7) \quad Q_{yx} = M\delta_{yx} - K_{yx},$$

<sup>2</sup>In three dimensions, the continuum limit of the staggered fermion action contains flavours corresponding to two inequivalent representations of the Dirac algebra [2].

where  $M$  is the fermion mass and  $K_{xy}$  is the *hopping matrix* that is non-zero for nearest neighbor pairs  $(x, y)$ . By inspection of (4), we write the quark matrix as

$$(8) \quad Q_{yx} = M\delta_{yx} - K \sum_{\mu=1}^D \alpha_{x\mu} (\delta_{y, x-\hat{\mu}} - \delta_{y-\hat{\mu}, x}).$$

We now apply a well known identity for the determinant of (any) matrix  $Q$ ,

$$(9) \quad \det Q = \sum_{\pi} \text{sgn}(\pi) \prod_x Q_{x\pi(x)},$$

where  $\pi$  ranges over the set  $\Pi$  of all permutations of the indices of  $Q$  and  $\text{sgn}(\pi)$  is the sign of the permutation. In the case of the quark matrix  $Q$ , the matrix indices being permuted correspond to vertices of the lattice. Thus, one is led to consider the product  $\prod_x Q_{x\pi(x)}$  for every permutation of lattice vertices.

The next step is to recognize that every permutation  $\pi$  can be decomposed into a composition of disjoint, non-trivial *cyclic* permutations  $\pi^c$ ,  $\pi = \prod_i \pi_i^c$ . For a matrix with all entries non-zero, these permutations may involve sets of vertices that are arbitrarily separated on the lattice. However, the quark matrices that arise in practice have a very specific structure (originating in the lattice discretization from nearest neighbor approximations of the derivative operator); the only non-zero matrix elements consist of nearest-neighbor pairs (and in the massive case, on-diagonal). Thus, the non-zero contributions can be analyzed as follows.

A given permutation  $\pi$  affects any vertex trivially (the vertex is sent to itself) or as part of a non-trivial cyclic permutation. In the massive case, vertices that are permuted trivially give *monomer* factors equal to the mass  $M$ . In the massless case where diagonal entries vanish, any trivial permutation will lead to a vanishing contribution; thus every vertex must participate in a cyclic permutation in the massless case.

For the non-trivial permutations, it is useful to distinguish two cases that a vertex may participate in. Permutations that swap a pair of neighboring vertices are referred to as *dimers*; all other non-trivial permutations consist of non-trivial loops of edges on the lattice; we shall refer to these as *cycles*. Given these observations on the structure of  $Q$ , we can now write an expression for  $\det Q$  in more explicit detail as

$$(10) \quad \det Q_{yx} = \sum_{\pi \in \Pi} \text{sgn}(\pi) M^{N_m} \prod_{(xy) \in p} K_{xy}.$$

Where  $N_m$  are the number of monomers. The product is over all directed edges  $(xy)$  that are part of a dimer or cycle of the permutation.

**2.2. Coupled case.** To couple fermions to the gauge fields, the ordinary derivative is replaced by the covariant one, thereby introducing the gauge variables  $g_e$  which act on the fermions through the matrices of the representation corresponding to the charge of the fermion. For specificity, we will consider fermions charged in the representation of  $G$  labelled by  $c$ . One can show [12] that the lattice action for staggered fermions coupled to the gauge field becomes

$$(11) \quad S = \sum_x \left( M(\bar{\psi}_x \psi_x) + K \sum_{\mu}^D \alpha_{x\mu} (\bar{\psi}_x U_{x\mu}^\dagger \psi_{x+\hat{\mu}} - \bar{\psi}_{x+\hat{\mu}} U_{x\mu} \psi_x) \right).$$

In contrast to the (simplified one component) free case, there is in general a vector possessing multiple Grassmann variable components at each vertex, and matrices  $U(g_e)$  that act non-trivially on this vector. In terms of our permutation expansion, the quark matrix now takes on component as well as vertex labels as follows:

$$(12) \quad S_F[g_e, \psi_v, \bar{\psi}_v] = \sum_{x, y \in V} \bar{\psi}_y^j Q[g_e]_{yx}^{ji} \psi_x^i.$$

Comparing (12) to (11) we identify the multicomponent quark matrix as

$$(13) \quad Q_{yx}^{ji}[g_e] = M\delta_{yx} - K \sum_{\mu=1}^D \alpha_{x\mu} ((U_{x\mu}^\dagger)^{ij} \delta_{y, x-\hat{\mu}} - (U_{x\mu})^{ij} \delta_{y-\hat{\mu}, x}).$$

The  $g_e$  dependence is through the representation matrices  $U_e$ , where  $e$  is labelled in one of the two conventions introduced above. The determinant formula can again be applied; upon doing so, the expansion into

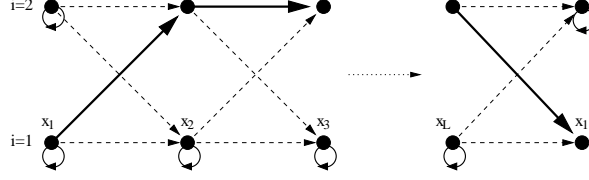


FIGURE 2. Graphical representation of one (solid) of all possible permutations (dashed) associated with a cycle of vertices of length  $L$ .

permutations takes on the form

$$(14) \quad \det Q[g_e] = \sum_{\pi} \text{sgn}(\pi) \prod_{x,i} Q_{x\pi_V(x,i)}^{i\pi_I(x,i)}.$$

Observe that the permutations  $\pi$  now act on both vertex and component indices of  $Q$ ; the action of  $\pi$  on indices and vertices can be separated into the maps  $\pi_I$  and  $\pi_V$ , respectively. As in the free case, the locality structure allows one to identify non-vanishing, polymer-like contributions. For  $\pi$  where vertex index mapping is trivial, the only non-vanishing entries are those for which  $\pi_I(x,i) = i$  as the massive term is an inner product with no cross-terms. Thus, the monomers contribute factors  $Mn$ , where  $n$  are the number of components of the fermion vectors.

As in the single-component case, for vertices that participate in non-trivial permutations, one still has that only permutations which move  $x \rightarrow \pi(x)$  where  $\pi(x)$  is a nearest neighbor are non-vanishing. However, due to the presence of multiple components to the fermion field, permutations can shift both components at a vertex simultaneously.

Configurations which involve non-trivial shifts of more than a single component (multiply occupied vertex contributions) are discussed in the Appendix B. In the remainder of this section, we will restrict ourselves to the case where only a single component participates in the shift, to illustrate in a simple setting how the trace of a product of  $U_e$  matrices comes about.

By inspection of (11), we see for a given nearest neighbor vertex shift, *all possible permutations of indices are allowed*, since in the general case  $U_{x\mu}^{ij}$  has all non-vanishing entries. To continue our analysis we factor the permutation into a part that acts on vertices  $\pi_V$  (these correspond to the dimers and cycles of the free case) and a part that acts on component indices  $\pi_I$ . We now write the fermion determinant as

$$(15) \quad \det Q[g_e] = \sum_{\pi_V} \text{sgn}(\pi_V) \sum_{\pi_I} \prod_x Q_{x\pi_V(x)}^{i\pi_I(x,i)} + (\text{multiply occupied vertex contributions}).$$

Focusing our attention on the first term, we note that only one component per vertex is shifted in each of the products of the sum (multiple component shifts at a vertex are precisely what is included in the second term, discussed in Appendix B). For a given  $\pi_V$ , we can represent  $\pi_I$  as an ordered sequence of arrows through the discrete  $n$ -point space living above every vertex acted on by  $\pi_V$ ; see Figure 2. Note that for a given dimer or cycle  $\pi_V$ , all possible index sequences correspond to permutations of the same order (thus  $\text{sgn}(\pi_V)$  can be factored out). The final step in the analysis is to recognize that the sum over all paths is simply the trace of the matrix product of representation matrices around the cycle.

We define  $D_1$  as the restriction of  $\det Q[g_e]$  to permutations involving singly occupied vertices; that is, the first term of (15).  $D_1$  can be constructed out of loops with a single associated trace as follows:

$$(16) \quad \begin{aligned} D_1 &= \sum_{\pi_V} \text{sgn}(\pi_V) \sum_{\pi_I} \prod_x Q_{x\pi_V(x)}^{i\pi_I(x,i)} \\ &= \sum_{\pi_V} \text{sgn}(\pi_V) (nM)^{N_m} K^{N_e} \left( \prod_{(xy) \in \pi_V} \alpha_{(xy)} \right) U_{(x_1 x_2)}^{i_1 i_2} U_{(x_2 x_3)}^{i_2 i_3} U_{(x_3 x_4)}^{i_3 i_4} \cdots U_{(x_L x_1)}^{i_L i_1} \\ &= \sum_{\pi_V} \text{sgn}(\pi_V) (nM)^{N_m} K^{N_e} \left( \prod_{(xy) \in \pi_V} \alpha_{(xy)} \right) \text{Tr} \left( \prod_{(xy) \in \pi_V} U_{(xy)} \right), \end{aligned}$$

where  $N_e$  is the total number of edges where vertices are shifted in the permutation. In the second line, the Einstein summation convention for repeated indices is used. Observe that  $(xy)$  denotes an oriented edge.

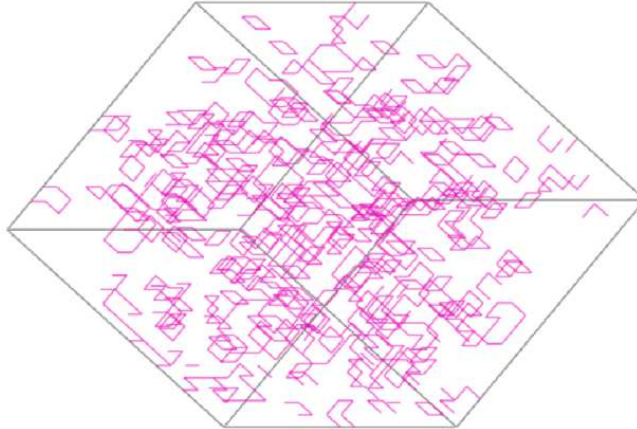


FIGURE 3. Visualization of 2-component fermion field on  $16^3$  lattice. Polymers that appear to have open ends close on the opposite side of lattice due to periodic boundary conditions.

Depending on whether  $(xy)$  is along or opposing the canonical orientation, one has either a product of  $U_{(xy)}$  or  $U_{(yx)} = U_{(xy)}^\dagger$ . The visualization of a typical polymer configuration on a  $D = 3$  lattice (including those with multiply occupied vertices) appears in Figure 3 below.

So far our discussion has been generic with regard to group, dimension, and fermion charge; the only major choice has been staggered fermions rather than an alternative lattice discretization. In the remainder of this work, we restrict our attention to  $D = 3$ ,  $G = SU(2)$ , and  $n$ -component massive fermion fields charged with half-integer spin  $c$  and minimally coupled to  $SU(2)$ .

### 3. SPIN FOAM DESCRIPTION OF PURE GAUGE THEORY ON THE LATTICE

Having described what we shall refer to as the free (no coupling to gauge fields) fermion partition function in terms of closed lattice polymers, in this section we briefly review the dual formulation of pure (no coupling to fermions) Yang-Mills, which leads to closed, colored, branched lattice surfaces. We shall see in the next section that these pictures naturally combine to give the full interacting partition function in terms of a space of coupled configurations.

It can be shown (see for example [3, 13], and [5] for detail on  $G = SU(2)$  in three dimensions) that starting from the lattice discretized action for pure Yang-Mills

$$(17) \quad \mathcal{Z}_B = \int \prod_{e \in E} dg_e e^{-\sum_{p \in P} S(g_e)},$$

one can transform to a spin foam formulation expressing the partition function in terms of dual variables as follows:

$$(18) \quad \mathcal{Z}_B = \sum_j \left( \sum_i \prod_{v \in V} 18j^v(i_v, j_v) \prod_{e \in E} N^e(i_e, j_e)^{-1} \right) \left( \prod_{p \in P} e^{-\frac{2}{\beta} j_p(j_p+1)} (2j_p + 1) \right).$$

Here  $V$ ,  $E$ , and  $P$  denotes the vertices, edges, and plaquettes of the lattice, respectively. The summations over  $i$  and  $j$  range over all possible edge and plaquette labellings, respectively. A plaquette labelling  $j$  assigns an irreducible representation of  $SU(2)$  to each element of  $P$ . These representations are labelled by non-negative half-integers (we will denote this set by  $\frac{1}{2}\mathbb{N}$ ), also referred to as *spins*; a labelling  $j$  is thus a map  $j: P \rightarrow \frac{1}{2}\mathbb{N}$ . In the  $SU(2)$ ,  $D = 3$  case, edges are also labeled by half-integer representations. thus an edge labelling is a map  $i: E \rightarrow \frac{1}{2}\mathbb{N}$ .

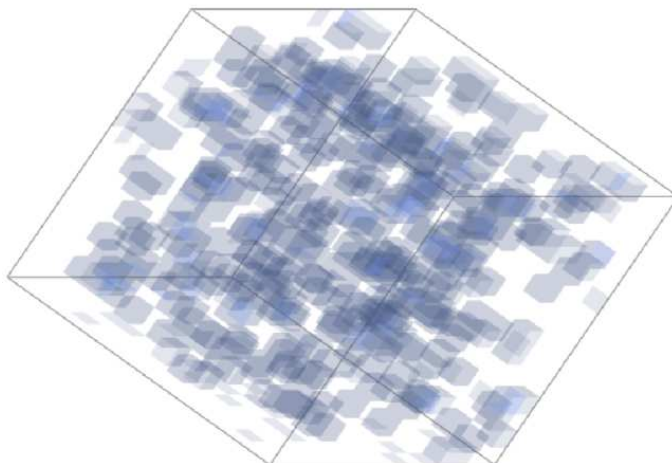


FIGURE 4. Visualization of pure Yang-Mills vacuum on  $16^3$  lattice.

Following [5], we define a (vacuum) *spin foam* configuration as one summand in (18), i.e. a labelling of both plaquettes and edges by spins and intertwiners, respectively. The amplitude assigned to a spin foam factors into a local product of amplitudes. The vertex amplitude ( $18j$  symbol) depends on the 12 plaquettes and 6 edges incident to a vertex; the  $N_e$  factors depend on the 4 plaquettes and the intertwiner labelling of an edge, and there is a product of local plaquette factors.

The locality of the spin foam formulation was applied in [5] to perform computations that were verified against conventional methods.

#### 4. DUAL FERMION-BOSON SIMULATIONS

In this section we describe how the dual pictures of lattice fermions and gauge bosons presented in the previous two sections can be combined to form a joint dual partition function, built up of gauge-invariant configurations with discrete occupancy and representation labels.

**4.1. The Joint Partition Function.** Using the action  $S[g_e, \psi_v, \bar{\psi}_v]$  for the full theory we write the partition function as follows:

$$\begin{aligned}
 (19) \quad Z_J &= \int \left( \prod_{e \in E} dg_e \right) \int \left( \prod_{v \in V} d\psi_v d\bar{\psi}_v \right) e^{-S_F[g_e, \psi_v, \bar{\psi}_v]} e^{-S_G[g_e]} \\
 &= \int \left( \prod_{e \in E} dg_e \right) \det Q[g_e] e^{-S_G[g_e]},
 \end{aligned}$$

where we have integrated out the fermionic variables to get the fermion determinant. We next use the polymer expansion for the determinant in the case of gauge-coupled  $Q$ , as described in Section 2.2:

$$\begin{aligned}
 (20) \quad Z_J &= \int \left( \prod_{e \in E} dg_e \right) \det Q[g_e] e^{-S_G[g_e]} \\
 &= \int \left( \prod_{e \in E} dg_e \right) \sum_{\gamma} \text{sgn}(\gamma) (nM)^{N_m} K^{N_K} \left( \prod_{(xy) \in \gamma} \alpha_{(xy)} \right) \text{Tr} \left( \prod_{(xy) \in \gamma} U_{(xy)} \right) e^{-S_G[g_e]}.
 \end{aligned}$$

Here  $N_K$  is the number of  $K$  factors (one per unit of edge occupancy) in the polymer configuration; the definition of polymer configuration for  $D = 3$ ,  $G = SU(2)$  is given in Section 4.3.1. In the second line, we

have substituted the polymer expansion for fermion determinant. Next, we recall the form of the character expansion (see [5] and references therein) for the amplitude based on the heat kernel action at a plaquette  $p$ ,

$$(21) \quad e^{-S_p(g)} = \frac{1}{K(I, \frac{\gamma^2}{2})} \sum_j (2j+1) e^{-\frac{\gamma^2}{2} j(j+1)} \chi_j(g), \quad j = 0, \frac{1}{2}, 1, \dots$$

Substituting the character expansion into the previous equation, we have

$$(22) \quad \mathcal{Z}_J = \int \left( \prod_{e \in E} dg_e \right) \sum_{\gamma} \text{sgn}(\gamma) (nM)^{N_m} K^{N_\kappa} \left( \prod_{(xy) \in \gamma} \alpha_{(xy)} \right) \text{Tr} \left( \prod_{(xy) \in \gamma} U_{(xy)} \right) \\ \times \prod_{p \in P} \sum_{j_p} (2j_p + 1) e^{-\frac{\gamma^2}{2} j_p(j_p+1)} \chi_{j_p}(g),$$

where an overall constant factor of  $K(I, \frac{\gamma^2}{2})$  per plaquette has been discarded. We show in Appendix A that the group integrals over products of traces and characters in each term of the character expansion can be evaluated exactly in terms of charged 18j symbols, provided a sum over intertwiner labels is made at each edge. Using the vertex and edge amplitudes of Appendix A, we can exhibit the joint dual partition function as

$$(23) \quad \mathcal{Z}_J = \sum_{\gamma \in \mathcal{P}} \sum_j \sum_i \left( s(\gamma) \prod_{v \in V} \overline{18j^v}(i_v, j_v, \gamma) \prod_{e \in E} \overline{N^e}(i_e, j_e, \gamma)^{-1} \prod_{p \in P} e^{-\frac{\gamma^2}{2} j_p(j_p+1)} (2j_p + 1) \right),$$

where  $s(\gamma) \equiv \text{sgn}(\gamma) \prod_{(xy) \in \gamma} \alpha_{(xy)} (nM)^{N_m} K^{N_\kappa}$  combines the two sign factors and a product of  $M$  and  $K$  factors. As we shall see in the next section, joint configurations associated to a polymer  $\gamma$  carry in general three rather than a single intertwiner label  $i_e$  for each edge belonging to the polymer;  $i$  here ranges over all the intertwiner labels.

Although the overall dual amplitude is still a product of local amplitudes as in the pure Yang-Mills case, the presence of the Wilson loop functionals associated to non-trivial polymers requires the vacuum vertex and edge amplitudes to be modified in a way that we define in Appendix A; the result is a product of modified  $\overline{18j^v}$  symbols and edge amplitudes  $\overline{N^e}$  that are charged according to the polymer content  $\gamma$  of the configuration.

The joint ensemble that results here can be viewed as a generalization of the usual definition of spin foams to include one-dimensional structure corresponding to the presence of fermionic charge. For a given polymer, there is a sum over all spin foams satisfying admissibility, which is modified at the polymer edges. From the worldsheet point of view [4], a polymer loop acts as the source or sink of  $2c$  fundamental sheets, where  $c$  is the half-integer charge of the fermion.

**4.2. The Joint Fermion-Boson Configurations.** In this section we define explicitly the set of configurations that include all those that give non-zero contributions<sup>3</sup> to the joint dual partition function.

Specifically, for a given polymer  $\gamma$ , we introduce definitions that will allow us to characterize the set of spin foam configurations (plaquette colorings) that are admissible in the presence of  $\gamma$ .

As in the pure Yang-Mills case [5], we assume a splitting has been made for each edge with  $j_1$  and  $j_2$  on one side and  $j_3$  and  $j_4$  on the other. Because of the presence of charges  $c_1$  and  $c_2$ , the intertwiner is generally 6-valent and three splittings have to be made. For discussing edge admissibility, we assume the splitting is such that  $c_1$  and  $c_2$  are in the middle of the channel as shown in Figure 5. Less symmetric splittings are possible, but we restrict our attention to this case in the following.

Let  $\gamma$  denote a polymer configuration of charge  $c$ . We define the set of  $\gamma$ -admissible plaquette configurations as those configurations whose labellings satisfy  $c$ -edge admissibility at every edge in the lattice, where  $c$ -admissibility is defined as follows:

**Definition 4.1** ( $c$ -edge admissibility). The spins assigned to plaquettes incident to an edge are said to be  $c$ -edge admissible if the *parity* and *triangle inequality* conditions are satisfied. The charge insertions  $c_1$  and

---

<sup>3</sup>Due to exceptional zeros there may be configurations that are admissible by the conditions defined in this section, but are nonetheless zero. As in the pure Yang-Mills case [5], we assume exceptional zeros are sufficiently isolated that ergodicity on admissibles is equivalent to ergodicity on non-zero configurations.



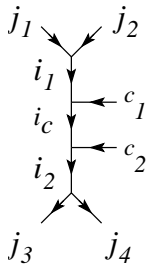


FIGURE 5. Symmetric splitting of a 6-valent  $SU(2)$  spin network vertex.

$c_2$  may be 0 or  $c$ , according to whether the edge is uncharged, singly charged, or doubly charged. Writing  $j_1, j_2, j_3$  and  $j_4$  for the four spins incident to a given edge, these conditions are

(1) **Parity:**

$$j_1 + j_2 + j_3 + j_4 + c_1 + c_2 \text{ is an integer.}$$

(2) **Triangle Inequality:** for each permutation  $x \equiv (x_1, x_2, x_3, x_4, x_5, x_6)$  of the charge and spin variables  $(c_1, c_2, j_1, j_2, j_3, j_4)$  we have

$$x_1 + x_2 + x_3 + x_4 + x_5 \geq x_6.$$

These conditions are equivalent to the existence of a non-zero invariant vector in the  $SU(2)$  representation  $c_1 \otimes c_2 \otimes j_1 \otimes j_2 \otimes j_3 \otimes j_4$ .

The allowed range of intertwiner labels  $i_1, i_c$  and  $i_2$  depend on the incident spin labels, on each other and on  $c$  through the vertices where the charges  $c_1$  and  $c_2$  enter the diagram. We now state the condition for an admissible spin foam (plaquette and edge intertwiner labelling) in the presence of an arbitrary polymer  $\gamma$ :

**Definition 4.2** ( $\gamma$ -admissible spin foam). A spin foam is  $\gamma$ -admissible if and only if for every edge  $e \in E$ :

- (1) The plaquettes incident to  $e$  are  $c$ -edge admissible in the sense of Definition 4.1, with  $c_1$  and  $c_2$  assigned depending on the occupancy of  $e$  by  $\gamma$ .
- (2) Each vertex of Figure 5 is admissible. Explicitly, the following conditions are simultaneously satisfied:

$$i_2 + j_1 + j_2, i_1 + i_c + c_1, i_2 + i_c + c_2 \text{ and } i_1 + j_3 + j_4 \text{ are integers}$$

and

$$i_1 \in [|j_1 - j_2|, j_1 + j_2] \cap [|i_c - c_1|, |i_c + c_1|],$$

$$i_c \in [|i_1 - c_1|, i_1 + c_1] \cap [|i_2 - c_2|, |i_2 + c_2|],$$

$$i_2 \in [|j_3 - j_4|, j_3 + j_4] \cap [|i_c - c_2|, |i_c + c_2|].$$

For a given polymer  $\gamma$ , we denote the set of  $\gamma$ -admissible spin foams by  $\mathcal{F}_\gamma^A$ .

**4.3. The Joint Moves and Algorithm.** In this section we define moves that transform from one joint configuration to another. Together, they are ergodic and obey detailed balance and can thus be used in a Metropolis or other Markov chain Monte Carlo algorithms.

**Definition 4.3** (Pure spin foam move). A pure spin foam move consists of a single application of the *cube*, *edge*, or *homology* move. In terms of their effect on plaquette spins, these moves are as defined in [5]. However, their effect on intertwiner labels needs to be generalized to account for the extra intertwiner labellings introduced by polymers.

Because polymer moves require simultaneous changes in spin foam structure, we use the term “pure” to distinguish spin moves that leave the polymer structure unchanged. We now describe the generalization of each pure spin foam move to account for extra intertwiner labels.

**Definition 4.4** (Generalized cube move). As described in Definition 2.4 and Appendix A.3 of [5]. With reference to compatible intertwiner moves of Type A, no changes in intertwiner labels are necessary. For Type B edges, all three labels are increased or decreased by the same half-unit of spin.

**Definition 4.5** (Generalized edge move). As described in Definition 2.5 of [5]. Rather than changing the single intertwiner label, the three intertwiner labels  $i_1(e)$ ,  $i_2(e)$  and  $i_c(e)$  are each randomly changed by  $-2, 0$ , or  $2$  (to preserve parity) units of spin.

**Definition 4.6** (Generalized homology move). As described in Definition 2.6 of [5], but all three intertwiner labels are increased or decreased by one half-unit of spin.

4.3.1. *Polymer moves.* In Section 2.2, we saw how sums over permutations in  $\Pi$  can be encoded into traces of matrix products, ordered according to the orientation of the permutation. Our example was restricted to singly occupied vertices, and is generalized in Appendix B. Combining these cases, we see that the sum over all permutations in  $\Pi$  can be represented by traces of products of matrices, if we include diagrams corresponding to all possible routings at multiply occupied vertices. This new set of objects, oriented diagrams with routings at multiply occupied vertices, we refer to as *polymers*, and denote by  $\mathcal{P}$ . It is important to distinguish the polymers from their finer-grained constituents, the permutations  $\Pi$ , as polymers can be coupled naturally into the spin foam partition function, whereas individual permutations cannot be using the methods here.

In this section we present a set of moves that are ergodic on the space of polymers  $\mathcal{P}$  on a 3-dimensional hypercubic lattice. The polymer states at an edge in the 2-component case considered here are as follows. Assuming a global orientation has been selected for the edges, an edge can be unoccupied, singly occupied, or doubly occupied with the occupied cases carrying both positive and negative orientation. The occupancy data at each edge can thus be assigned from the set  $\{-2, -1, 0, 1, 2\}$ . We shall use the term “line of flux” interchangeably with directed polymer line.

**Definition 4.7** (Plaquette move). A plaquette and plaquette orientation (clockwise or counterclockwise) is randomly selected. To each edge, a delta occupancy of  $+1$  or  $-1$  (with signs given according to plaquette orientation) is assigned, and added to the present occupancy. If the resulting occupancy on any edge has magnitude greater than 2, the move is immediately rejected. At each multi-valent vertex, a choice of routing is made with equal probability. A proposed move that removes occupancy of edges incident on multiply occupied vertices must make further random choice of routing that matches the routing present or be rejected. This is necessary to preserve detailed balance. If the move is not rejected, the spin of the selected plaquette is randomly decreased or increased by  $c$  to satisfy parity. Because a change in the polymer occupancy forces a change in both the plaquette spin and the charge structure at an edge, the affected intertwiner labels (at each edge of the affected plaquette) must change in a way that is compatible; if not the result will be immediately  $c$ -edge inadmissible for the new charging.

This is the most fundamental polymer-changing move, and connects a very large region of the space of polymers contributing to the fermion determinant. One can see trivially that the plaquette move can create fundamental loops of either orientation when applied to “empty” space (plaquettes of zero occupancy edges). Figure 6 illustrates how the plaquette move can deform an existing cycle. The same plaquette move of opposite orientation would lead to one of multiple routings with a doubly occupied edge, as shown by Figure 10 in Appendix B.

Because an equally weighted routing choice is made amongst several alternatives when the plaquette move of (for example) Figure 10 is made, the move that reverses a particular routing to get the initial loop back should occur with proportional probability, in order to satisfy detailed balance. This will unfortunately lead to a lowered acceptance rate, particularly in regimes with high occupancy.

To identify intertwiner moves compatible with a plaquette move, one must give the choice of splitting (grouping of  $j_1, \dots, j_4$  into pairs) around the edges of a plaquette, in the same way that intertwiner moves compatible with a cube move depends on the splitting (see A.3 of [5]). For conciseness and generality, we have made the present definition of the algorithm splitting independent. Forthcoming work on numerical simulations with this algorithm will evaluate alternative splittings and describe the appropriate compatible moves.

**Definition 4.8** (Global circle move). For integer valued charge  $c$ , a global circle moves adds a single line of charge and a minimal cylinder of  $\frac{c}{2}$  charged plaquette spins spanning the lattice. The origin and orientation of the cylinder is randomly selected to lie on a plaquette of one of three orthogonal lattice planes through the origin.

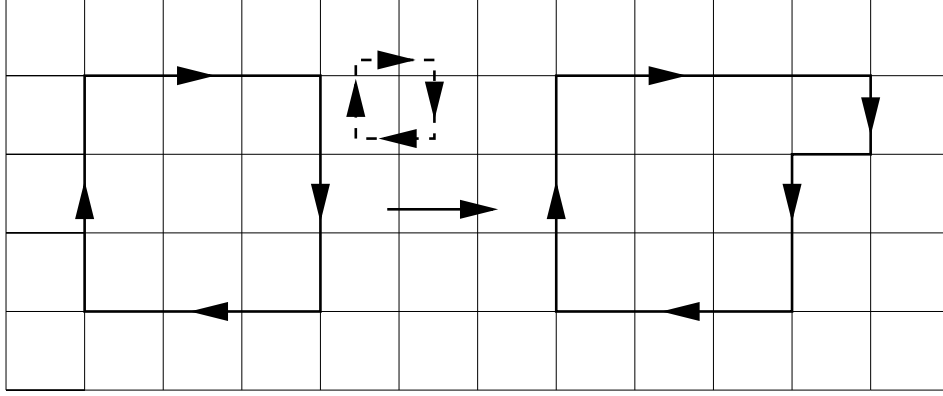


FIGURE 6. Stretching of a loop by a plaquette move

For half-integer  $c$ , two lines of charge spanning the lattice are added and a minimal surface consisting of a line of  $c$ -charged plaquettes is added between the charge lines. The position and orientation of the sheet is randomly selected to lie on an edge of one of the three orthogonal lattice planes through the origin.

As in the pure gauge theory case, the non-trivial global topology of lattices with periodic boundary conditions leads one to moves that create and destroy structure on a global scale, in this case lines of charge.

In the half-unit charge case, a second line needs to be added to absorb the flux introduced by the first; the “smallest” possible global move places a second line of half-unit charge immediately beside the first.

In the case of integer valued charge, the lowest energy (and hence smallest change in amplitude) structure satisfying admissibility is formed by wrapping the smallest possible cylinder supported by the lattice; because there are  $2n$  fundamental irreps,  $n$  can be incident on one side normal to the line, wrap into a cylinder, and enter the other to satisfy  $c$ -edge admissibility.

**Definition 4.9** (Dimer move). An edge is randomly selected and a single unit of occupancy is added or removed. If the result is not consistent with the presence of dimers and cycle edges (i.e. a cycle that ran through the edge is broken by the removal of occupancy), the move is rejected.

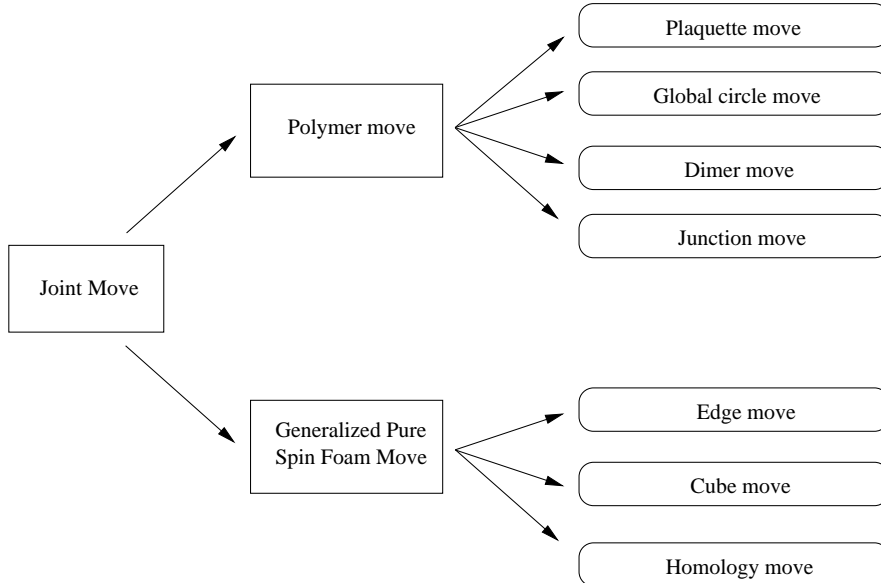
Singly and doubly charged dimers cannot be constructed by plaquette moves. Note a singly charged dimer contributes  $\text{Tr}(U_e U_e^\dagger) = n$  with weight  $K^2$  while a doubly charged dimer contributes  $\text{Tr}(U_e U_e^\dagger) \text{Tr}(U_e U_e^\dagger) - \text{Tr}(U_e U_e^\dagger U_e U_e^\dagger) = n^2 - n$  with weight  $K^4$  (unlike general polymers, we combine the two routings into one configuration). Both types of dimers evaluate to constants with respect to the gauge variables, and thus don't couple to the gauge bosons.

**Definition 4.10** (Junction move). A vertex is randomly selected, and if multiply occupied, the routing of flux is changed.

A multiply occupied vertex in the case of a 2-component fermion field has two flux paths, which can be routed in two different ways. When a multiply occupied vertex first appears as a result of a polymer move, one routing is randomly selected (similarly in the inverse case, with weightings to preserve detailed balance as discussed above). Thus, the junction moves are strictly speaking unnecessary for ergodicity, but may be used to improve performance of Metropolis algorithm.

4.3.2. *The Algorithm.* Combining the polymer and spin foam moves, given, we give a statement for a Metropolis algorithm ergodic on the joint ensemble.

**Algorithm 4.11.** (*Joint Fermion-Boson Algorithm*). An iteration of the joint algorithm consists of choosing one of the seven previously defined moves, which can be organized as follows:



The algorithm can be tuned to improve acceptance rate by adjusting the relative frequency of the attempted move types.

The algorithm also tracks the sign of the configuration changes with the creation and destruction of fermion loops, which can occur with any of the polymer moves. The product of monomer factors  $M$  and hopping factors  $K$  are also updated for polymer moves. It is important to emphasize that changes in both the sign and other factors require only local consideration of the polymer moves.

With regard to locality, one sees that the (pure spin foam) homology move and global circle moves will lead to updates costing on the order of  $L^2$  and  $L$  respectively, where  $L$  is a characteristic side length of the lattice. In the pure Yang-Mills case analyzed numerically in [5], the homology moves have negligible influence beyond very small lattice sizes. It remains to be seen how this is modified in the joint case, and how large an influence the global circle moves have.

Within the scope of the current work, the expectation values of observables depending on dual degrees of freedom are computed in the usual manner, by averaging the observable over the Markov chain generated by the Metropolis algorithm. For Wilson loop type observables commonly studied, the expectation value is actually a ratio of dual charged and dual vacuum partition functions, with static charge corresponding to the Wilson loop observable present in the charged partition function and a vacuum partition function given by  $\mathcal{Z}_J$  of equation (23). The computation of Wilson loop observables of pure Yang-mills and dynamical fermions will be reported on in forthcoming work by the author.

## 5. OUTLOOK AND CONCLUSIONS

We present here a local, exact algorithm for Metropolis simulation of the fermion-boson vacuum. The details have been provided for the case of  $D = 3$  staggered Kogut-Susskind fermions coupled to a Yang-Mills  $SU(2)$  field; however the algorithm has a straightforward generalization to other dimensions and gauge groups.

A limitation of the algorithm as currently given is the species doubling inherent in the (unrooted) Kogut-Susskind formulation (e.g. in four dimensions there will be four species). An alternative to Kogut-Susskind fermions which addresses species doubling was developed by Aroca et al. [1] and Fort [7]. We are currently investigating this modified fermion action in the non-abelian, higher dimensional context. Another approach would be to go through a similar procedure using Wilson fermions, in which the unwanted doublers become very heavy in the continuum limit.

The crucial question for any new fermion algorithm is its performance relative to the highly evolved dynamic fermion methods that exist within the conventional lattice gauge community today. In three-dimensions, slow-down at weaker coupling has been observed in recent work on the pure Yang-Mills case [5].

The situation in  $D = 4$  is not well understood and is currently the subject of numerical work by the author, as are improvements in the original  $D = 3$  case.

With regard to the continuum limit, we expect the most critical question for the algorithm proposed here is the seriousness of the sign problem. A hard sign problem has been discussed as a general feature of the polymer expansion in the continuum (small mass) limit [11]. While oscillating signs can be overcome for lattice fermions in certain two dimensional theories [11, 15], the author is not aware of methods that have successfully addressed the sign problem for  $D > 2$ . As both the fermion and dual Yang-Mills (spin foam) amplitudes can carry negative signs, an important question is how the signs interact; i.e. the problem of signs may be harder or easier than for either the free fermion polymer expansion or dual Yang-Mills alone, depending on how the signs correlate.

Although numerical developments are required to begin evaluating this proposal, we believe the approach may be of considerable interest. We find it remarkable that the fermion expansion into polymers and the gauge field dualization into spin foams (both of which have been extensively explored on their own), combine together in a way that is very compelling geometrically, and allows a local, exact Metropolis simulation using gauge-invariant configurations carrying entirely discrete labels.

*Acknowledgement.* The author would like to thank Dan Christensen, Florian Conrady, and Igor Khavkine for valuable discussions. The author was supported by NSERC.

## APPENDIX A. CHARGED $nJ$ SYMBOLS

**A.1. The dual model with charges.** In this appendix, we deal specifically with  $D = 3$ ,  $G = SU(2)$ . Following the discussion in the appendix of [5], we recall that the dual partition function (in the absence of charge) has the form

$$(24) \quad \mathcal{Z} = \sum_{\{j_p\}} \int \prod_{e \in E} dg_e \prod_{p \in P} c_{j_p} \chi_{j_p}(g_p),$$

where summation over  $j_p$  is over unitary irreducible representations of  $SU(2)$ . At this point it is convenient to specialize to a  $D = 3$  cubic lattice with periodic boundary conditions; orientation choice is as given in the appendix of [5]. With this choice of orientation, the holonomy around a plaquette  $p$  is  $g_p = g_1 g_2 g_3^{-1} g_4^{-1}$ , where  $g_1, g_2, g_3$  and  $g_4$  are the group elements associated to the edges of the plaquette  $p$ , starting with an appropriate edge and going cyclically. Recall that the inverse  $g_i^{-1}$  is used if the orientation of edge  $i$  does not agree with that of  $p$ . Thus

$$(25) \quad \chi_{j_p}(g_p) = U_{j_p}(g_1)_a^b U_{j_p}(g_2)_b^c U_{j_p}(g_3^{-1})_c^d U_{j_p}(g_4^{-1})_d^a,$$

where  $U_j(g)_a^b$  denotes a matrix element with respect to a basis of the  $j$  representation. If we insert (25) into (24) and collect together factors depending on the group element  $g_e$ , we get a product of independent integrals over the group, each of the form

$$(26) \quad \int dg_e U_{j_1}(g_e)_{a_1}^{b_1} U_{j_2}(g_e)_{a_2}^{b_2} U_{j_3}(g_e^{-1})_{a_3}^{b_3} U_{j_4}(g_e^{-1})_{a_4}^{b_4} = \int dg_e \begin{array}{c} \leftarrow \textcircled{g_e} \leftarrow j_1 \\ \leftarrow \textcircled{g_e} \leftarrow j_2 \\ \rightarrow \textcircled{g_e^{-1}} \rightarrow j_3 \\ \rightarrow \textcircled{g_e^{-1}} \rightarrow j_4 \end{array}.$$

Here and below we use a graphical notation for tensor contractions, as in [5].

Equation (26) defines a projection operator on the space of linear maps  $j_4 \otimes j_3 \rightarrow j_1 \otimes j_2$ , so it can be resolved into a sum over a basis of intertwiners  $I_i : j_4 \otimes j_3 \rightarrow j_1 \otimes j_2$

$$(27) \quad \int dg_e \begin{array}{c} \leftarrow \textcircled{g_e} \leftarrow j_1 \\ \leftarrow \textcircled{g_e} \leftarrow j_2 \\ \rightarrow \textcircled{g_e^{-1}} \rightarrow j_3 \\ \rightarrow \textcircled{g_e^{-1}} \rightarrow j_4 \end{array} = \sum_i \frac{I_i I_i^*}{\langle I_i^*, I_i \rangle} = \sum_i \frac{\begin{array}{c} j_1 \leftarrow \\ j_2 \leftarrow \\ j_3 \leftarrow \\ j_4 \leftarrow \\ \bullet \\ I_i \\ \bullet \\ j_1 \leftarrow \\ j_2 \leftarrow \\ j_3 \leftarrow \\ j_4 \leftarrow \end{array}}{\begin{array}{c} j_1 \leftarrow \\ j_2 \leftarrow \\ j_3 \leftarrow \\ j_4 \leftarrow \\ \bullet \\ I_i \\ \bullet \\ j_1 \leftarrow \\ j_2 \leftarrow \\ j_3 \leftarrow \\ j_4 \leftarrow \end{array}},$$

where the intertwiners  $I_i^* : j_1 \otimes j_2 \rightarrow j_4 \otimes j_3$  are chosen such that the trace  $\langle I_i^*, I_i \rangle$  of the composite  $I_i^* I_i$  is zero whenever  $i' \neq i$  and non-zero if  $i' = i$ . The projection property is readily verified.

We next define  $\mathcal{Z}_\gamma$ , the partition function charged according to the polymer  $\gamma$ , as follows

$$(28) \quad \mathcal{Z}_\gamma = \sum_{\{j_p\}} \int \prod_{e \in E} dg_e \text{Tr} \left( \prod_{e \in \gamma} U_c^e(g_e)_{i_e^-}^{i_e^+} \right) \prod_{p \in P} c_{j_p} \chi_{j_p}(g_p).$$

Collecting matrix factors by dependence on edge variable  $g_e$ , we find in addition to the matrices from the four incident plaquettes, a matrix from the edge  $e$  with charge  $c$  belonging to the polymer  $\gamma$ :<sup>4</sup>

$$(29) \quad \int dg_e U_{j_1}(g_e)_{a_1}^{b_1} U_{j_2}(g_e)_{a_2}^{b_2} U_{j_3}(g_e^{-1})_{a_3}^{b_3} U_{j_4}(g_e^{-1})_{a_4}^{b_4} U_c^e(g_e)_{i_e^-}^{i_e^+} = \int dg_e \begin{array}{c} \leftarrow \textcircled{g_e} \leftarrow j_1 \\ \leftarrow \textcircled{g_e} \leftarrow j_2 \\ \leftarrow \textcircled{g_e} \leftarrow c \\ \rightarrow \textcircled{g_e'} \rightarrow j_3 \\ \rightarrow \textcircled{g_e'} \rightarrow j_4 \end{array}.$$

As in the pure case, the group integral can be resolved into invariant intertwiners

$$(30) \quad \int dg_e \begin{array}{c} \leftarrow \textcircled{g_e} \leftarrow j_1 \\ \leftarrow \textcircled{g_e} \leftarrow j_2 \\ \leftarrow \textcircled{g_e} \leftarrow c \\ \rightarrow \textcircled{g_e'} \rightarrow j_3 \\ \rightarrow \textcircled{g_e'} \rightarrow j_4 \end{array} = \sum_i \frac{I_i I_i^*}{\langle I_i^*, I_i \rangle} = \sum_i \begin{array}{c} \begin{array}{c} j_1 \leftarrow \\ j_2 \leftarrow \\ c \leftarrow \\ j_3 \rightarrow \\ j_4 \rightarrow \end{array} \begin{array}{c} I_i \\ I_i^* \end{array} \begin{array}{c} \leftarrow j_1 \\ \leftarrow j_2 \\ \leftarrow c \\ \rightarrow j_3 \\ \rightarrow j_4 \end{array} \\ \begin{array}{c} \leftarrow j_1 \\ \leftarrow j_2 \\ \leftarrow c \\ \rightarrow j_3 \\ \rightarrow j_4 \end{array} \begin{array}{c} I_i \\ I_i^* \end{array} \begin{array}{c} \leftarrow j_1 \\ \leftarrow j_2 \\ \leftarrow c \\ \rightarrow j_3 \\ \rightarrow j_4 \end{array} \end{array}.$$

If, for each edge of the lattice, we fix a term  $i$  in the above summation, the intertwiners  $I_i$  and  $I_i^*$  can be contracted with those coming from the other edges, leading to a sum over intertwiner labellings at every edge. Observe that at edges occupied by polymers, there is more than a single intertwiner spin label due to the additional splittings (see Figure 5) introduced by the charge lines. At each vertex of the lattice, there will be six intertwiners  $I_i$  (some carrying multiple labels), and their contraction can be graphically represented as an octahedral network plus additional lines depending on how the polymer passes through the vertex. As well, at each edge there will be a normalization factor corresponding to the denominator of equation (30).

We consider first the vacuum case. In this case, each edge carries only a single intertwiner label. The result is the  $18j$  symbol central to pure Yang-Mills spin foams,

$$(31) \quad \begin{array}{c} +z \\ \diagup \quad \diagdown \\ \leftarrow \quad \rightarrow \\ \diagdown \quad \diagup \\ -x \\ \diagup \quad \diagdown \\ \leftarrow \quad \rightarrow \\ \diagdown \quad \diagup \\ +x \quad +y \\ \diagdown \quad \diagup \\ -z \end{array}.$$

The vertices are labelled by the directions of the associated lattice edges emanating from the given lattice vertex, namely  $\pm x$ ,  $\pm y$ , and  $\pm z$ . The value of the  $18j$  symbol depends on the choice of basis elements  $I_i$  and  $I_i^*$  in (30), the six summation indices  $i$  labelling the edges, and the 12 incident plaquette labels  $j$ .

We now turn to the case where there is a (single) polymer along one or more of the edges incident to a vertex. Each charged normalization factor  $\overline{N} \equiv \langle I_i^*, I_i \rangle$  in the denominator of (27) depends on the charge  $c$  of the fermion at that edge, the intertwiner labels  $i$  on that edge, and the labels of the four plaquettes incident on that edge. In the presence of external charges, the vacuum  $18j$  is modified depending on whether

<sup>4</sup>In the case where an edge is doubly occupied, the integral involves a sixth matrix (and the resolving intertwiners an additional input and output arrow). It is straightforward to generalize the present analysis to this case; the resulting doubly charged  $18j$  symbols are shown in Appendix B.

the line of charge proceeds directly through the vertex or turns, leaving in a direction perpendicular to entry direction. We call these cases *charged*  $18j$  symbols and denote them by an overline,  $\overline{18j}(j_v, i_e, \gamma)$  where the additional dependence on gamma reflects how the polymer charge is routed through the octahedral network. Typical charged  $18j$  symbols are shown in Figure 7. Cases where the direction of the arrow on the charged

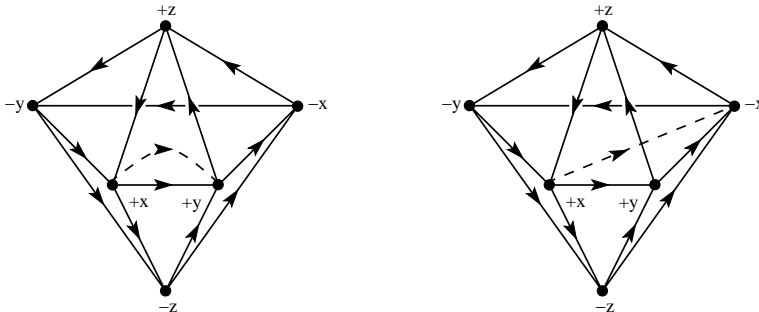


FIGURE 7. Charged  $18j$  symbols with flux lines passing through at right angles (left) and straight through (right).

lines is flipped will also occur, depending on the polymer orientation. Additionally, as discussed in the next section, more than a single line of flux can pass through a vertex, leading to charged  $18j$  symbols of the form shown in Figures 8 and 11.

In implementing numerical code for this algorithm, a choice of splitting (grouping of the four plaquettes into  $(j_1, j_2)$  and  $(j_3, j_4)$  pairs on opposite sides of the splitting) is made and each vertex resolved into a 3-valent sub-network with up to three non-trivial intertwiner labels, as shown in Figure 5. At this point, recoupling moves (see A.2 of [5], and references therein) can be used to reduce the spin network to sums and products of known spin networks such as the  $6j$  and theta networks, for which efficient algorithms are available. It should be noted, however, that different splittings lead to differing efficiency in implementation, so some care and experimentation should be applied to finding an efficient splitting. Specific splitting schemes and their performance evaluation will be reported on in forthcoming numerical work by the author and collaborators.

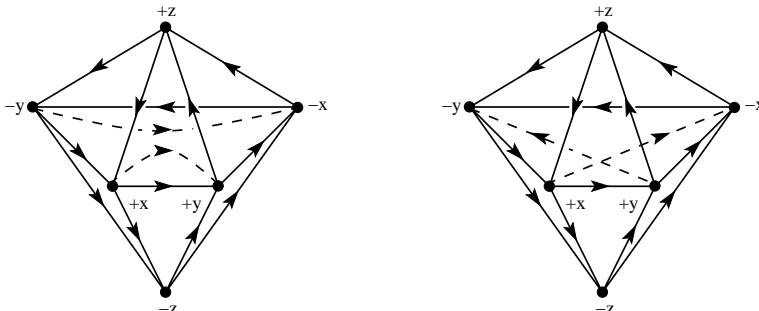


FIGURE 8. Charged  $18j$  symbols with two pairs of flux. Cases with flux not in the same plane are also possible.

## APPENDIX B. POLYMERS WITH MULTIPLY OCCUPIED VERTICES

In order to couple to the spin foam representation of the gauge theory, we seek to collect the permutation contributions to the fermion determinant into traces of products of  $U_e$  matrices around closed, oriented loops of edges. The case of permutations where a single component is shifted was discussed above in Section 2.2. For polymers where more than one component is shifted at a vertex, recovering a trace formula is somewhat more subtle.

In Figure 9, we illustrate a case where a vertex is multiply occupied; the orientation is such that there are two possible routings that resolve the ambiguity at that vertex. Neither diagram by itself corresponds to the desired sum of permutation contributions. In the matrix multiplications and traces (viewed as a sum

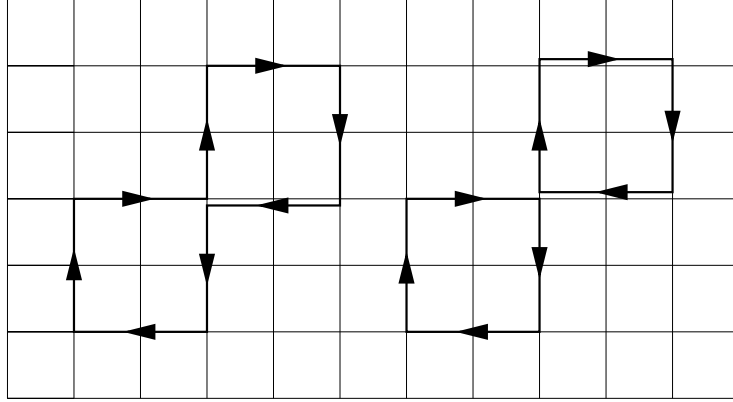


FIGURE 9. Two routings associated with a polymer that self intersects once at a point.

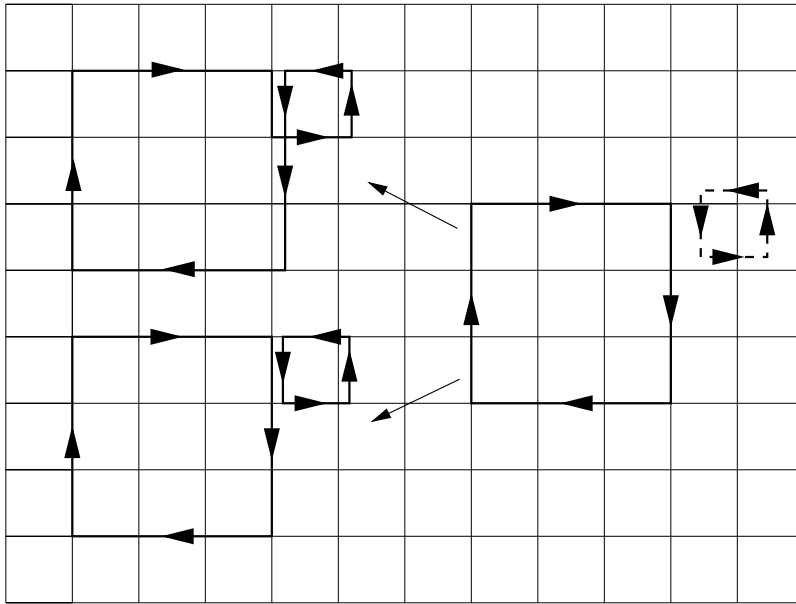


FIGURE 10. A move introducing a doubly occupied edge, for which there are two distinct routings.

over all paths around a loop), there are terms in each corresponding to paths that are not permutations. However, the same undesired terms occur with opposite sign in the two diagrams (as one involves paths that form a single loop, the other paths that lie in two disjoint loops) so the sum of both captures the sum of permutations associated with the polymer.

A similar cancellation occurs when two loops share a single edge, i.e. the edge is multiply occupied. Because there are two multiply occupied vertices, there are  $2^2 = 4$  routings possible, however only two are topologically distinct; two representatives appear in Figure 10. The cancellation of unphysical paths between the traces over differently routed polymers is well known from the hopping parameter expansion (HPE) of the fermion determinant as discussed for example in [14]. As shown in Figure 11, the presence of a doubly charged edge leads to a charged  $18j$  spin network with a 6-valent node. As well, the charged normalization factor  $\bar{N}$  on a doubly charged edge is as given in the denominator of equation (27), but with an additional  $c$ -charged line parallel to the original  $c$ -charged line.



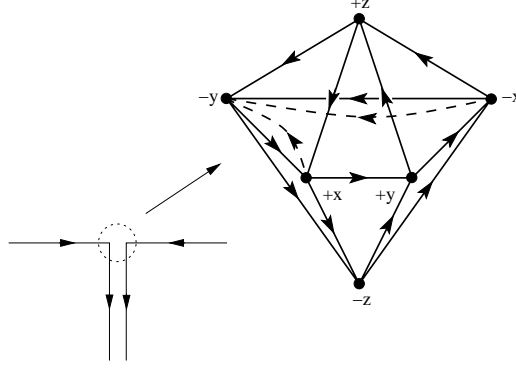


FIGURE 11. A charged 18j symbol containing a 6-valent node incoming from a doubly charged edge.

### REFERENCES

- [1] J. M. Aroca, H. Fort, R. Gambini. “Worldsheet formulation for lattice staggered fermions” (1997), arXiv:hep-lat/9607050v2.
- [2] C. Burden, A.N. Burkitt. “Lattice Fermions in Odd Dimensions” (1987), *Europhys. Lett.* **3**, 545–552.
- [3] F. Conrady. “Geometric spin foams, Yang-Mills theory, and background-independent models” (2005), arXiv:gr-qc/0504059v2.
- [4] F. Conrady, I. Khavkine. “An exact string representation of 3d SU(2) lattice Yang–Mills theory” (2007), arXiv:0706.3423v1 [hep-th].
- [5] J.W. Cherrington, J.D. Christensen, I. Khavkine. “Dual Computations of Non-abelian Yang-Mills on the Lattice” (2007), arXiv:0705.2629 [hep-lat]. To appear in *Phys. Rev. D*.
- [6] T. DeGrand, C. DeTar. *Lattice Methods for Quantum Chromodynamics* (2006), World Scientific, Singapore.
- [7] H. Fort. “The Worldsheet Formulation as an Alternative Method for Simulating Dynamical Fermions” (1997), *Phys.Lett. B* **444**, 174–178.
- [8] L. Kauffman, S. Lins. *Temperley-Lieb Recoupling Theory and Invariants of 3-Manifolds* (1994), Annals of Mathematics Studies, No. 134. Princeton University Press, New Jersey.
- [9] M. Karowski, R. Schrader, H.J. Thun. “Monte Carlo simulations for quantum field theories involving fermions” (1985), *Comm. Math. Phys.* Volume 97, Number 1, 5–29.
- [10] I. Montvay. “Bosonized dynamical fermions in 3+1 dimensions” (1989), *Physics Letters B* **227**, 375–380.
- [11] I. Montvay. “Simulation of staggered fermions by polymer algorithms” (1990), In *Probabilistic methods in quantum field theory and quantum gravity* (1990), Plenum Press, New York.
- [12] I. Montvay, G. Munster. *Quantum Fields on the Lattice* (1994), Cambridge University Press, Cambridge.
- [13] R. Oeckl, H. Pfeiffer. “The dual of pure non-Abelian lattice gauge theory as a spin foam model” (2001), *Nucl. Phys. B* **598**, 400–426.
- [14] H.J. Rothe. *Lattice Gauge Theories: An Introduction* (1992), World Scientific.
- [15] U. Wolff. “Cluster simulation of relativistic fermions in two space-time dimensions” (2007), arXiv:0707.2872v2.